Rotated Wedge Averaging Method for Junction Characterization*

Weichuan Yu, Kostas Daniilidis, Gerald Sommer
Institute of Computer Science
Christian Albrechts University
Preusserstrasse 1-9, D-24105 Kiel, Germany
Email: wy@informatik.uni-kiel.de

Abstract

The computational cost of conventional filter methods for junction characterization is very high. This burden can be attenuated by using steerable filters. However, in order to achieve a high orientational selectivity to characterize complex junctions a large number of basis filters is necessary. From this results a yet too high computational effort for steerable filters. In this paper we present a new method for characterizing junctions which keeps the high orientational resolution and is computationally efficient. It is based on applying rotated copies of a wedge averaging filter and estimating the derivative with respect to the polar angle. The new method is compared with the steerable wedge filter method [13] in experiments with real images. We show the superiority of our method as well as its adaptability to scale changes and robustness against noise.

1 Introduction

Junctions of gray-value lines or edges are rare events in images carrying important information for many image processing tasks like point matching in object recognition, point tracking in motion analysis and attentive coding.

In order to use junctions for such tasks we must be able to locate their corresponding keypoints, to characterize them by means of signatures and to classify them in junction categories. Regarding keypoint detection and localization the reader is referred to Foerstner's study [4] and to the comparison of different operators by Rohr [11, 12]. In this paper we address the problem of junction characterization. The resulting signature can be used for further junction classification.

*The financial support of the first author by DAAD (German Academic Exchange Service) and of the second and third author by DFG grant 320/1-2 is greatly acknowledged. We thank Dr. H. Farid for his helpful discussions and for providing the programs of the steerable wedge filter.

Junctions are local gray-value structures with multiple intrinsic scales and orientations. A signature characterizing such a junction can be only obtained by applying a filter in different scales and orientations. This leads to an enormous computational load. For example, in order to extract orientational information of a junction in conventional filter methods we have to rotate the same filter repeatedly. For an angle field of 360° and a sampling interval of 10° already 36 rotated copies of the original filter should be applied. In order to reduce this effort, the concept of steerability is introduced [5, 9].

A steerable filter is synthesized/approximated as a linear combination of a finite set of so-called basis filters. It can interpolate any arbitrary rotational angle. Usually the number of basis filters is much less than that of rotations. Therefore the computational cost is highly reduced.

Many kinds of steerable filters are used to characterize junctions. Freeman and Adelson [5] steered derivatives of the 2D Gaussian filter to analyze orientation. These kernels are exactly steerable, but they have poor orientational selectivity. Moreover, they are either symmetric or antisymmetric [13]. This results in a period of 180° in orientation and leads to an ambiguity in responses between terminating and non-terminating junctions. Perona [10] applied the elongated Gaussian-derivative kernels to achieve high orientational selectivity. Though such kernels are not exactly steerable, the best approximations are guaranteed by using singular value decomposition (SVD). In addition, Perona generalized the steerability from orientation to a set of parameters like position and scale. Michaelis and Sommer [7] proposed a method for junction characterization based on SVD. The steered filter was a double Hermite function composed of the second (real part) and first (imaginary part) derivative of a 2D elongated Gaussian function. By applying the associated one-sided function their method does not suffer from the 180° period ambiguity.

Recently, Simoncelli and Farid [13] proposed a steerable wedge filter for local orientation analysis. This exactly steerable filter is designed in the polar coordinate system. It looks like a wedge in radial direction and its angular part is synthesized by Fourier series. The usage of angular Fourier series brings two improvements compared with the Gaussian-derivative kernels used by Freeman and Adelson [5]: First, there is no more symmetric ambiguity because the wedge kernel is asymmetric in angle. Secondly, high orientational selectivity can be achieved by using many angle harmonics. Steerable wedge filters extend the notion of exact steerability to non-derivative based filters and present a more general set of steerable filters exceeding the conventional convergence of Gaussian shaped kernels.

Steerability provides us with a solid mathematical theory to analyze orientation, scale and other image parameters [9, 1, 2]. In addition, it has been integrated with other theories such as Lie group theory [8] and invariance theory [3] for special purposes. However, the complexity of its implementation remains high. Due to the uncertainty principle the product of orientational resolution of a steerable filter and its orientational bandwidth has a lower bound. Therefore, in order to achieve a high orientational selectivity we have to apply a too large number of basis filters [9, 7] with large spatial support.

In order to characterize the keypoint with low computational cost we apply rotated copies of a filter with small spatial support directly. In the frame of steerability this would be a serious limitation for the choice of filters. But the frame of steerability is too general with respect to junction characterization. Furthermore, we try to accomplish all filtering by avoiding 2D convolution which is computationally expensive.

This paper is organized as follows: In section 2 we describe the Rotated Wedge Averaging Method (*RWAM*) in detail. In section 3 we compare the complexity of the steerable wedge filter [13] with our approach and we show the performance of both filters in real experiments. Finally, we discuss some further modifications needed to improve the new method.

2 Rotated Wedge Averaging Method

Our method applies a local polar mapping at a keypoint: $f(x,y) \rightarrow f(\rho,\phi)$. A wedge with a constant angle width is defined to have its origin at the keypoint and expand in radial direction till a fixed radius. Then, we estimate the averaging value in the wedge support as shown in figure 1. We rotate this wedge around the keypoint gradually and after each rotation the mean gray value of the wedge is computed. For a wedge centered at θ only pixels with their coordinates satisfying $\rho \leq R$ and $|\phi - \theta| \leq \frac{W}{2}$ can be involved into the computation. The positions of local maxima show the orientation of lines and the positions of steepest descent/ascent indicate the orientation of edges. Because edges are more important than lines we further apply an 1D derivative filter with respect to the angle to get the required information. In this paper we use the first derivative of an 1D Gaussian function(G_1). Thus, for a circular neighborhood of a keypoint $f(x,y)$ the impulse response yields:

$$h(\theta) \stackrel{def}{=} \mid \frac{d}{d\theta} Gauss(\theta) * g(\theta) \mid \qquad (1)$$

with

$$g(\theta) \stackrel{def}{=} \frac{1}{\mathcal{N}(f(\rho,\phi))} \sum_{\rho=0}^{R} \sum_{\phi=\theta-\frac{W}{2}}^{\theta+\frac{W}{2}} f(\rho,\phi) \qquad (2)$$

where $\mathcal{N}(\,)$ means the number of pixels in the mask and $\theta \in [0, 2\pi]$. The maxima of $g(\theta)$ and $h(\theta)$ indicate the existence of lines and edges, respectively.

The algorithm is described in detail as follows:

Step 1. Fix parameters: radius of wedge R (pixel), wedge width W (degree), rotation step $\delta\theta$ (degree) and size of G_1 filter S (tap).

Step 2. Set the angle $\theta = 0°$.

Step 3. Determine the wedge according to R,W and θ. Its form is shown in figure 1.

Step 4. Calculate the mean gray value of the corresponding wedge as the averaging value at θ.

Step 5. $\theta = \theta + \delta\theta$

Step 6. If $\theta < 360°$ go to Step 3, otherwise get the entire *averaging output* $g(\theta)$.

Step 7. Apply G_1 on the 1D *averaging output* and take absolute values of results as the *differentiation output* $h(\theta)$.

One drawback of the grid representation of images is that we have different numbers of pixels in wedges at different angles, even though we have defined a constant angle width criterion. This can be demonstrated in the following example: In a circle with $R = 15$ pixels, a digital line passing through the center at 0° contains $2R + 1 = 31$ pixels while a line passing through the center but at 45° has only $int(\frac{2R}{\sqrt{2}}) = 21$ pixels. To reduce this harmful effect we choose mean gray values in wedges as outputs.

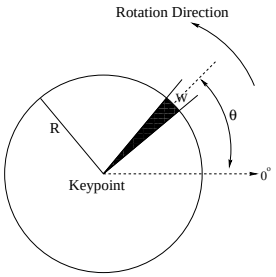

Figure 1: The wedge in *RWAM*, R is radius of the wedge, W is wedge width. Keypoint is at the center of the circle. The arrow shows the direction to rotate the wedge.

In figure 2 we apply *RWAM* on line junctions. The junction is characterized by the maxima of the $g(\theta)$ function illustrated more intuitively in the right column of the figure. In figure 3 we show the performance on edge junctions. In addition, *RWAM* performs very well in the presence of noise (see figure 4).

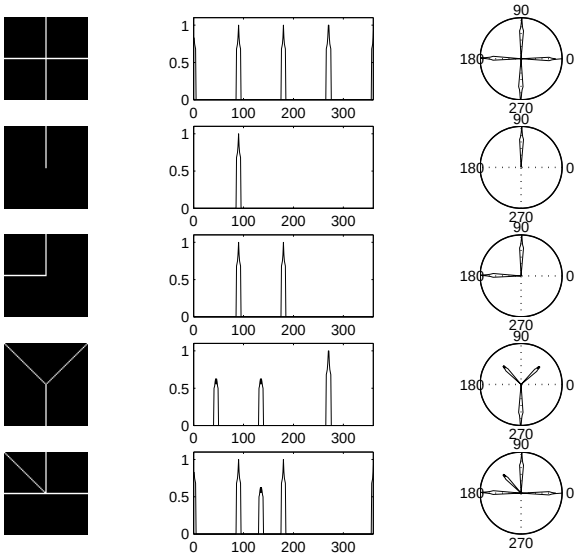

Figure 2: **Left:** Synthetic line junction images with the size of 65×65 pixels and line width of 1 pixel. **Middle:** *Averaging outputs* $g(\theta)$ v.s. θ from $0°$ to $360°$. $W = 8°$, $R = 15$. The positions of the local maxima exhibit the orientations of lines. **Right:** Corresponding polar plots of the results in the middle column. The numbers around circles are angles in degree.

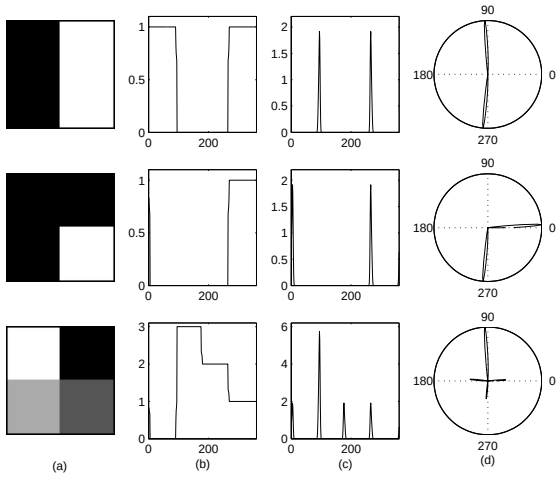

Figure 3: **(a):** Synthetic edge junctions. **(b):** *Averaging outputs* $g(\theta)$ (θ from $0°$ to $360°$). $W = 8°$, $R = 15$. **(c):** *Differentiation outputs* $h(\theta)$ applying 11-tap G_1 filter. Note that they are absolute values of the differentiations. **(d):** Corresponding polar plots of column (c). The small deviations in orientations result from the fact that an edge can only be presented by two pixels in the grid, while we can not set the center of a wedge between two pixels.

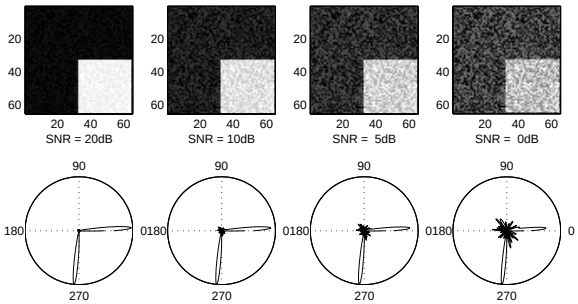

Figure 4: **Top:** A synthetic edge junction disturbed by incremental random noise. **Bottom:** Corresponding *Differentiation outputs* $h(\theta)$. Even in the very noisy case ($SNR = 0dB$) we can still match the junction. $W = 10°$, $R = 9$, $S = 11$.

3 Comparisons and Real Experiments

Many kinds of steerable filters are used to analyze junctions. Since the steerable wedge filter [13] represents basic attributes of steerable filters and has a similar wedge shape like the wedge in *RWAM*, we choose this filter for comparison.

Steerable filter methods are based on convolution. The computational cost is proportional to the num-

ber of basis filters. In order to implement the steerable wedge filter [13] with N basis filters of tap size P we require $N(P^2 + \frac{360^\circ}{\delta\psi})$ multiplications and $N(P^2-1) + \frac{360^\circ}{\delta\psi}(N-1)$ additions, where $\delta\psi$ is the sampling interval in the angle domain. Our *RWAM* is a sampling method and we must choose a small sampling interval (an angle step of 1° is fine enough to characterize *all* possible junctions) in order to extract local structure information. The complexity reduction is two-fold. First, we apply filters with much smaller support than the basis filters in [13]. Secondly, due to averaging we have up to the Gaussian derivative with respect to the angle only additions and about 360 multiplications.

It should be noticed that the local polar mapping can be done "off-line" since it is a transform between coordinates and is therefore valid for all different images. The resulting look-up-table (LUT) is of negligible complexity in comparison to the averaging step.

Precisely, to employ *RWAM* we need addition, multiplication and division. Addition is used in calculating averaging values and in applying G_1. Its amount A is a function of W, $\delta\theta$, R and S. Taking the overlapping of adjacent wedges into account we have:

$$A = \frac{W}{\delta\theta}\pi(R+1)^2 + \frac{360^\circ}{\delta\theta}(S-1) \qquad (3)$$

We need M multiplications for 1D differentiation:

$$M = \frac{360^\circ}{\delta\theta}S \qquad (4)$$

To estimate mean gray values in wedges we calculate also divisions with the complexity D:

$$D = \frac{360^\circ}{\delta\theta} \qquad (5)$$

Because multiplication and division have the same calculating complexity M and D can be merged.

In order to compare computational complexities, the radial expansion of masks in [13] and our method should be the same so that the following relation is satisfied: $P = 2R + 1$. Both sampling intervals are designed to be identical as well: $\delta\psi = \delta\theta = 1^\circ$. Therefore we need totally $N(P^2+360)$ multiplications and $N(P^2-1)+360(N-1)$ additions in the steerable wedge filter[13] and $M+D = 360(S+1)$ multiplications and $W\pi(R+1)^2+360(S-1)$ additions in *RWAM*. Though the computational cost of these two methods are functions of different parameters, we can compare them by studying the effort to achieve the same resolution.

Figure 5 is such an example. To achieve the equivalent orientational selectivity, 45 basis filters, totally 59445 multiplications and 59040 additions ($N = 45, P = 31$) are required in the steerable wedge filter method [13], while using *RWAM* we compute only 4320 multiplications and 6817 additions ($W = 4^\circ, R = 15, S = 11$). From this comparison we can draw a conclusion that *RWAM* is more efficient to achieve high resolution. Moreover, the computational load is even lower at higher resolution, i.e., at smaller W in *RWAM*. This property is very attractive if we note that in the steerable wedge filter [13] higher angle resolution always results in a higher number N of basis filters.

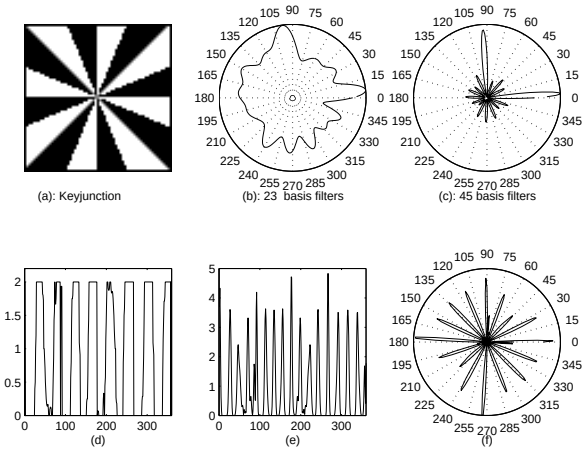

Figure 5: **(a):** Binary Siemens star with 16 edges spanning roughly evenly in the orientation space. **(b):** Polar plot of the result using the steerable wedge filter [13] composed of 23 basis filters with 31-tap size. We can not see orientations of edges correctly. **(c):** The same as in (b) but using 45 basis filters. The orientations of edges can be seen now. The strange performance of the steerable wedge filter [13] is due to the angular aliasing effect in the mask. **(d):** *Averaging output* $g(\theta)$ using *RWAM* with $W = 4^\circ$, $R = 15$. **(e):** *Differentiation output* $h(\theta)$ of *RWAM* with $S = 11$. **(f):** Polar plot of (e). The orientations of the edges are clearly presented.

Beside the computational efficiency *RWAM* is also adaptable to scale variations. It is known that all filters are sensitive to scale changes [6]. For instance, a wide line will be recognized as two edges by filters with small scale. In filter methods we need to introduce scale steerability to cope with this modification [10]. This results in even more computations. However, *RWAM* can adapt the scale variations by adjusting W straightforwardly (s. figure 6). A set of wedges with different W can further be used to characterize junctions from small to large scales.

The scale of steerable wedge filters [13] is inversely proportional to the orientational selectivity. It should be adapted for scale changes in a similar way. But in [13] quadratic filters are used such that they have the same responses for lines and edges. This is not suitable for describing scale changes.

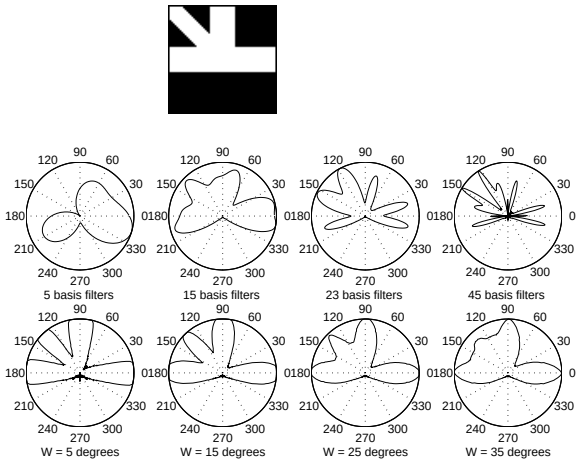

Figure 6: *RWAM* is adaptable to scale changes. **Top:** A junction with line width of 15 pixels. **Middle:** Responses of steerable wedge filters [13] with different number of basis filters. With the increase of basis filters the angle resolution rises. But the lines are recognized as edges due to their intrinsic structures. **Bottom:** *Averaging outputs* of *RWAM* with different W. The positions of the orientational maxima are more and more accurate with the increase of W. At $W = 25°$ we can get the desired representation. Of course if W is too big, the angle resolution will be damaged, just like demonstrated at $W = 35°$.

We have seen the successful behavior of *RWAM* on synthetic junction characterization. In the following real experimental results are presented. In figure 7 we show the high orientational selectivity of *RWAM*. While the steerable wedge filter [13] detects only the dominant dark line between the lips of Lena, *RWAM* recognizes different orientations of her two lips. This information can be very useful in face recognition. In figure 8 we show junctions with textural neighborhood. The effect of texture is illustrated by the ripples in $g(\theta)$ in the middle row which can lead to many local maxima in $h(\theta)$ due to the derivative. In order to attenuate such ripples we set larger W and S in our method. Another real example of edge junctions is presented in figure 9. In comparison to the steerable wedge filter [13] with 30 basis filters our method characterizes the directions of junctions more distinctively but is relatively sensitive to high frequency components due to the derivative.

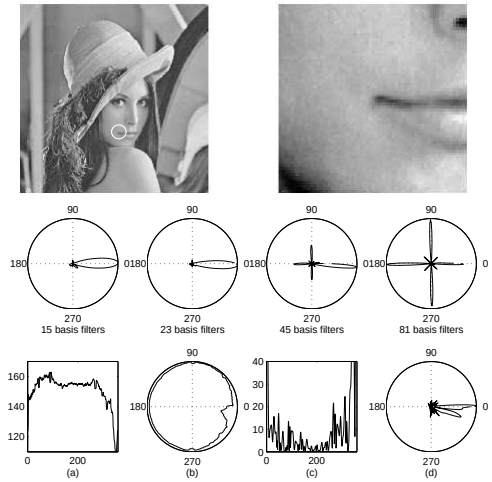

Figure 7: Comparison of resolutions between steerable wedge filter [13] and *RWAM*. **Top Left:** The famous image "Lena" with her lips corner as a keypoint. **Top Right:** Lips corner in detail. **Middle:** Polar plots using the steerable wedge filter [13] with different number of basis filters. Only the dominant dark line between the lips can be recognized. **Bottom (a) (b):** Plot and polar plot of the *averaging output* of *RWAM*. $W = 5°, R = 15$. The dark line is clearly to see as a notch in (b). **Bottom (c) (d):** Plot and polar plot of *the differentiation output* of *RWAM*. The orientations of two lips are distinct in (d). G_1 with larger size ($S = 17$) is used to smooth the noise in the *averaging outputs*. The computational cost rises a little as price.

4 Conclusion and Further Work

In this paper we have presented a new approach to characterize junctions. The computational complexity is reduced by applying wedge filters with smaller support and by replacing 2D convolution with additions and 1D convolution. Traditional steerability is based on the approximation by a Fourier series. Our approach approximates the variation with respect to orientation by applying the convolution with a smoothing filter. We are on the way to provide the mathematical background for such an approximation. Further, we argue that the orthogonality relation among different basis functions like in the Fourier theory may be not an essential condition for signal reconstruction.

Further work includes the study of the influence of the keypoint offset as well as the substitution of the

averaging filter with a Gaussian function as a smoothing filter with a reasonable complexity increase.

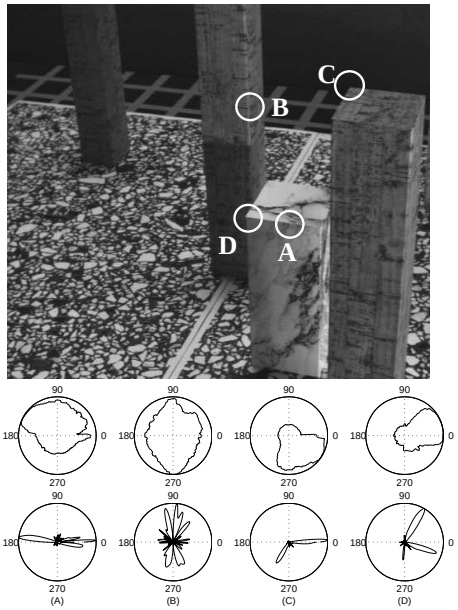

Figure 8: **Top:** "Block world" image. The junctions are marked with letters. A:horizontal edge; B: vertical line; C: 'L' edge junction; D: 'T' edge junction. **Middle:** *Averaging outputs* $g(\theta)$ of *RWAM*. **Bottom:** *Differentiation outputs* $h(\theta)$. For B we get its orientation information directly from the middle row. For A, C *and* D we get their orientation information from the bottom row. It is worth mentioning that in D although the dark edge near 270° is very blurred, *RWAM* can still address it. $W = 10°, R = 9, S = 17$.

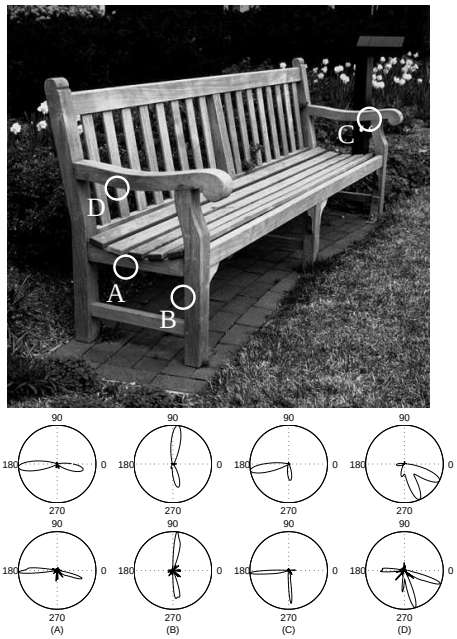

Figure 9: **Top:** Parkbench with marked edge junctions. A: horizontal edge; B:vertical edge; C: corner; D: 'T' junction. **Middle:** Steerable wedge filter results using 30 basis filters. $P = 19$. **Bottom:** $h(\theta)$ of *RWAM*. All junctions are matched. $W = 10°, R = 9, S = 21$.

References

[1] E.P. Simoncelli, W.T. Freeman, E.H. Adelson and D.J. Heeger. Shiftable multi-scale transforms. *IEEE Trans. Information Theory*, 38(2):587–607, 1992.

[2] D. H. Ballard and L. E. Wixson. Object recognition using steerable filters at multiple scales. In *IEEE Workshop on Qualitative Vision*, pages 2–10, 1993.

[3] W. Beil. Steerable filters and invariance theory. *Pattern Recognition Letters*, 15:453–460, 1994.

[4] W. Foerstner. A framework for low level feature extraction. In *European Conf. on Computer Vision*, volume II, pages 383–394, Stockholm, Sweden, May 2-6, J.O. Eklundh (Ed.), Springer LNCS 801, 1994.

[5] W.T. Freeman and E.H. Adelson. The design and use of steerable filters. *IEEE Trans. Pattern Analysis and Machine Intelligence*, 13:891–906, 1991.

[6] J.J. Koenderink and A.J. van Doorn. Generic neighborhood operators. *IEEE Trans. Pattern Analysis and Machine Intelligence*, 14(6):597–605, 1992.

[7] M. Michaelis and G. Sommer. Junction classification by multiple orientation detection. In *European Conf. on Computer Vision*, volume I, pages 101–108, Stockholm, Sweden, May 2-6, J.O. Eklundh (Ed.), Springer LNCS 800, 1994.

[8] M. Michaelis and G. Sommer. A Lie group approach to steerable filters. *Pattern Recognition Letters*, 16:1165–1174, 1995.

[9] P. Perona. Deformable kernels for early vision. In *Conference on Computer Vision and Pattern Recognition*, pages 222–227, Maui, Hawaii, June 3-6, 1991.

[10] P. Perona. Steerable-scalable kernels for edge detection and junction analysis. *Image and Vision Computing*, 10(10):663–672, 1992.

[11] K. Rohr. Recognizing corners by fitting parametric models. *International Journal of Computer Vision*, 9(3):213–230, 1992.

[12] K. Rohr. On the precision in estimating the location of edges and corners. *Journal of Mathematical Imaging and Vision*, 7:7–22, 1997.

[13] E. P. Simoncelli and H. Farid. Steerable wedge filters for local orientation analysis. *IEEE Trans. Image Processing*, 5(9):1377–1382, 1996.